

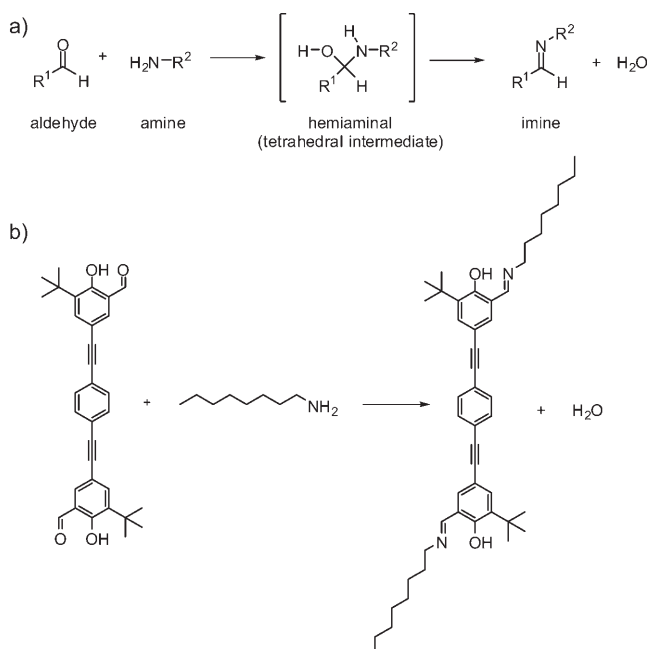
# Covalent Interlinking of an Aldehyde and an Amine on a Au(111) Surface in Ultrahigh Vacuum\*\*

Sigrid Weigelt, Carsten Busse, Christian Bombis, Martin M. Knudsen, Kurt V. Gothelf,\*  
Thomas Strunskus, Christof Wöll, Mats Dahlbom, Bjørk Hammer, Erik Lægsgaard,  
Flemming Besenbacher, and Trolle R. Linderoth\*

Organized molecular structures are central to the formation of advanced functional surfaces in the field of nanotechnology. The principles of supramolecular chemistry have recently been applied extensively to molecules adsorbed at surfaces under ultrahigh-vacuum (UHV) conditions, and complex molecular structures formed by self-assembly based on weak, reversible interactions, such as van der Waals forces,<sup>[1]</sup> dipole–dipole interactions,<sup>[2]</sup> hydrogen bonding,<sup>[3,4]</sup> or metal complexation,<sup>[5]</sup> have been revealed by using local-probe scanning tunneling microscopy (STM). Similar studies on the covalent interlinking of molecules adsorbed directly on surfaces under UHV conditions have been surprisingly scarce. Chemical reaction has been induced locally with the STM tip,<sup>[6]</sup> and a few cases of monocomponent polymerization have been reported,<sup>[7]</sup> but in several instances compounds anticipated to react under normal solution conditions have been shown to instead form structures based on noncovalent interactions.<sup>[4,8]</sup> Herein, we perform a two-component condensation reaction between aldehydes and amines coadsorbed on a Au(111) surface, and investigate the conformation and lateral ordering of the imine reaction products by submolecular-resolution STM. Covalent interlinking is confirmed by comparison to the

STM signature of the reaction product formed ex situ, as well as by near-edge X-ray absorption fine structure (NEXAFS) spectroscopy. A solvent-free reaction path, based solely on internal proton transfers, is proposed from ab initio density functional theory (DFT) calculations.

Imines are of fundamental importance in synthetic chemistry, and the basic reaction mechanism for their formation from an aldehyde and an amine is shown in Scheme 1 a.<sup>[9]</sup> Thin films of imines<sup>[10]</sup> and imides<sup>[11]</sup> have been



**Scheme 1.** a) Generalized solution-catalyzed formation of an imine from an aldehyde and an amine. b) Thermally induced reaction between a dialdehyde and octylamine coadsorbed on a Au(111) surface in UHV.

grown on surfaces by vapor deposition polymerization. In our study of imine formation at the extreme low-coverage limit from reactants coadsorbed directly on an inert herringbone-reconstructed Au(111)-(22 × √3) surface under UHV conditions, we used the dialdehyde and the aliphatic amine shown in Scheme 1 b. Similar salicylaldehyde-derived compounds are known to react in solution with amines to form imines.<sup>[12]</sup>

The dialdehyde molecules adsorb with their backbones parallel to the substrate and form well-ordered structures of monomolecular height (Figure 1 a).<sup>[13]</sup> The molecular top-

[\*] M. M. Knudsen, Prof. K. V. Gothelf  
Danish National Research Foundation: Centre for DNA Nanotechnology at iNANO and Department of Chemistry  
University of Aarhus (Denmark)  
Fax: (+45) 8619-6199  
E-mail: kvg@chem.au.dk  
Dr. S. Weigelt, Dr. C. Busse, Dr. C. Bombis, Dr. M. Dahlbom,  
Prof. B. Hammer, Prof. E. Lægsgaard, Prof. F. Besenbacher,  
Prof. T. R. Linderoth  
Interdisciplinary Nanoscience Center (iNANO), and Department of  
Physics and Astronomy  
University of Aarhus (Denmark)  
Fax: (+45) 8942-3690  
E-mail: trolle@inano.dk  
Dr. C. Busse, Dr. T. Strunskus, Prof. C. Wöll  
Lehrstuhl für Physikalische Chemie I  
Ruhr-Universität Bochum, 44780 Bochum (Germany)

[\*\*] We acknowledge financial support from the EU programs FUN-SMART and PICO-INSIDE, as well as from the Carlsberg Foundation, the Danish Technical and Natural Science Research Councils, and the Danish National Research Foundation. We thank A. H. Thomsen and M. Nielsen for their help with the synthesis of the molecules. We acknowledge fruitful discussions with C. Schalley and G. Witte.

Supporting information for this article is available on the WWW under <http://www.angewandte.org> or from the author.

ography is typically dominated by bright protrusions at the ends of the molecules arising from the *tert*-butyl groups. Octylamine forms a densely packed lamellar structure as shown in Figure 1 b.

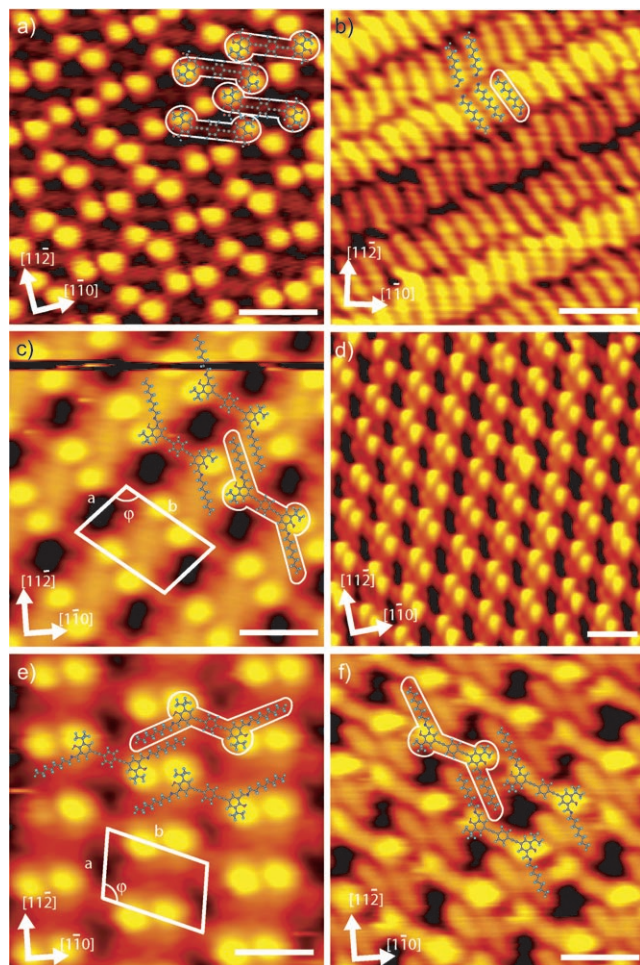


**Figure 1.** STM images of reactants and products in the reaction of Scheme 1 b on a Au(111) surface. The molecular structures are overlaid and outlined on certain images. a) Self-assembled island formed by the dialdehyde ( $V_t = -1.0$  V,  $I_t = -0.77$  nA, bar size 2 nm). b) Lamellar structure formed by octylamine ( $V_t = +2.0$  V,  $I_t = 0.41$  nA, bar size 2 nm). c) Self-assembled structure formed by the diimine prepared in situ at room temperature ( $V_t = +1.9$  V,  $I_t = 0.27$  nA, bar size 2 nm). The unit cell of the structure is indicated. d) Large ordered domain formed by the diimine prepared in situ and annealed at 450 K ( $V_t = -2.2$  V,  $I_t = -0.42$  nA, bar size 4 nm). e) Self-assembled structure formed by the diimine prepared ex situ and dosed onto a sample at 120 K ( $V_t = -2.0$  V,  $I_t = -0.29$  nA, bar size 2 nm). The unit cell of the structure is indicated. f) Self-assembled structure formed by the diimine prepared ex situ and observed in the backbone-imaging mode ( $V_t = +1.9$  V,  $I_t = 0.38$  nA, bar size 2 nm).<sup>[13]</sup>

To perform the 2D surface reaction, the dialdehyde was first deposited on the Au(111) substrate to create a submonolayer coverage of molecular islands. Subsequently, the surface was brought close to saturation of the first monolayer by exposing it to a vapor of octylamine ( $p \approx 1\text{--}5 \times 10^{-8}$  mbar),

while the sample was held at room temperature ( $T \approx 300$  K). This procedure resulted in a highly ordered structure (Figure 1 c), different from the structures formed by exposing the surface to the individual reactants. The protrusions in the STM images associated with the *tert*-butyl groups form parallel double rows with the aromatic backbone visible between two bright protrusions belonging to neighboring rows. Features with a length matching the length of the octylamine molecule extend from the aromatic end group from the side opposite to the *tert*-butyl group, that is, from the position originally occupied by the aldehyde group. Alkyl chains from adjacent molecules align pairwise, similarly to the lamellar motif observed for the octylamine structure. All these STM features for the codeposited molecular structure are consistent with it being formed by the diimine product, as overlaid in Figure 1 c. To confirm this hypothesis, the diimine was synthesized ex situ by conventional solution-phase techniques and was subsequently evaporated onto a gold substrate held at a temperature of approximately 120 K to prevent thermally activated on-surface reactions. Adsorption of the ex situ reaction product indeed resulted in small structural domains (Figure 1 e) identical to those observed after surface reaction (Figure 1 c). Figures 1 c,e depict mirror domains constructed from opposite surface enantiomers of the diimine, as clarified by the overlaid structures. The dimensions of the unit cells for the in situ and ex situ structures are identical within experimental error ( $a = (16.9 \pm 0.9)$ ,  $b = (26.8 \pm 1.3)$  Å,  $\phi = (107 \pm 3)^\circ$ ), with the aromatic backbones tilted at an angle  $\angle b, \langle 110 \rangle = (25 \pm 4)^\circ$  with respect to the nearest close-packed direction of the Au(111) surface. We can, thus, conclude that the structures resulting from diimines formed in situ and ex situ are identical. In Figure 1 f, the structure is shown in an STM imaging mode that suppresses the bright *tert*-butyl,<sup>[13]</sup> thereby highlighting the positions of the aromatic backbone and alkyl chains. The positions of the alkyl chains with respect to the aromatic backbone match the expected conformation of the diimine product, which is stabilized by an intramolecular hydrogen bond between the imine nitrogen atom and the hydroxy group.

Annealing the molecular surface structures at 400–450 K led to larger ordered domains of diimine molecules, as observed for products formed both in situ (Figure 1 d) and ex situ, signaling completion of the reaction, increased surface mobility, and possibly also switching of the molecular conformation<sup>[13]</sup> at this elevated temperature. Upon deposition of the diimine formed ex situ, we also observed free amines on the substrate, indicating either some fragmentation upon evaporation or the presence of surplus amines in the molecular powder.

To obtain spectroscopic confirmation that an in situ 2D surface reaction had occurred, we performed NEXAFS spectroscopy studies. Carbon 1s spectra of the reactants and of the ex situ and in situ products on the Au(111) surface are shown in Figure 2. The peak at  $E_{\pi 1^*} = 284.9$  eV is attributed to a superposition of peaks arising from carbon atoms on the aromatic backbone<sup>[14]</sup> and is shared by the dialdehyde and the ex situ and in situ reaction products. As expected, this peak is absent for the octylamine, which only shows a broad resonance arising from  $\sigma$  orbitals of the alkyl chains. The

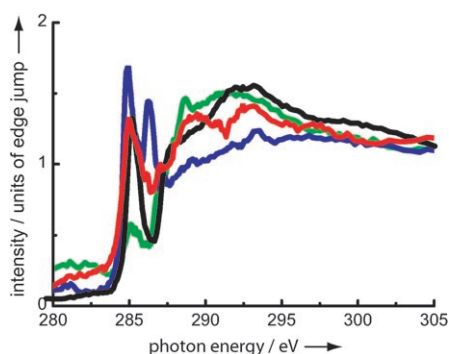


**Figure 2.** Carbon 1s NEXAFS spectra of octylamine (green), the dialdehyde (blue), the diimine prepared ex situ (black), and the diimine prepared in situ (red). The spectra were obtained at an incidence angle of 30°.

peak at  $E_{\pi 2^*} = 286.3$  eV stems from the carbon atom in the aldehyde group,<sup>[14]</sup> and is present for the dialdehyde and absent for the ex situ product, which does not contain an aldehyde group. For the in situ product (red curve), the aldehyde peak is significantly reduced, which is the expected spectroscopic signature for the formation of the imine. A peak for the imine carbon atom is not observed in the spectrum, as it is presumably superimposed on the peaks arising from the aromatic carbon atoms.<sup>[15]</sup>

It is surprising that the imine formation proceeds under the extreme UHV conditions, because in the conventional reaction scheme (Scheme 1a), the last step, in which the tetrahedral intermediate is converted into the imine product, is normally catalyzed by the solvent, which acts as a combined proton donor/acceptor. To establish a plausible reaction path in the absence of a solvent, state-of-the-art, ab initio DFT calculations were performed (Figure 3). To reduce the computational load, the amine and the dialdehyde were cut off beyond the reacting groups and saturated with hydrogen atoms, as shown in the starting configuration **1**. In the first step of the reaction path, the amino group undergoes a nucleophilic addition to the carbonyl group with formation of the tetrahedral hemiaminal intermediate **2**. Next, the phenol hydroxy group donates a proton to the hydroxy group of the hemiaminal, and water is eliminated, configuration **3**. Finally, a rotation around the bond between the phenyl ring and the iminium carbon atom takes place (see Figure S1 in the Supporting Information), and the iminium group donates a proton to the phenoxy group (configurations **4–6**). In this reaction pathway, all energy barriers are less than 1.17 eV, enabling the reaction to proceed at the annealing temperature of 400 K (an Arrhenius expression gives 0.02 reaction events per second with a prefactor of  $10^{13} \text{ s}^{-1}$ ). Experimentally, we observed that formation of the imine also proceeds at room temperature. This observation indicates the existence of a more favorable energy pathway or reduced energy barriers caused by catalytic effects of the underlying metal substrate. An important feature of the proposed reaction mechanism is that the phenol hydroxy group acts as an internal proton donor/acceptor and, thereby, substitutes for the solvent present under normal solution-phase conditions. Direct conversion of the tetrahedral intermediate into the imine product

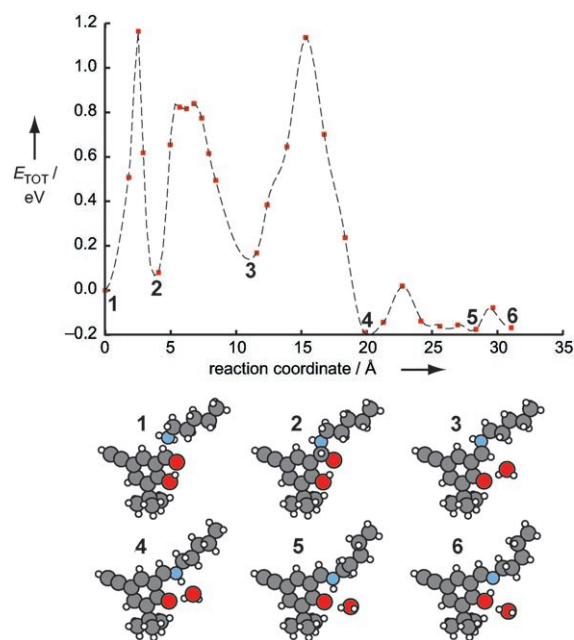


**Figure 3.** Optimum reaction pathway identified by theoretical modeling. The numbers on the graph correspond to the molecular conformations shown below the graph. See text for details.

in the absence of a proton-donor/acceptor group has previously been shown to result in an energy barrier of approximately 2.4 eV,<sup>[16]</sup> which would make the reaction unlikely at moderate temperatures.

In summary, we have covalently interlinked an aldehyde and an amine coadsorbed on a Au(111) surface under UHV conditions. The imine reaction product was observed by STM to form laterally ordered structures similar to those obtained from the product synthesized ex situ. The results offer new prospects for the formation of laterally ordered surface nanostructures or polymers of high thermal and chemical stability through interlinking by strong covalent bonds, as opposed to the weaker, reversible interactions underlying molecular self-assembly on surfaces.

## Experimental Section

The STM experiments were performed in a UHV system equipped with a noncommercial variable-temperature Aarhus STM (see also <http://www.specs.de>).<sup>[17]</sup> The Au(111) surface was prepared by argon-ion sputtering at 1.5 kV followed by annealing at 850 K. Details on the synthesis of the dialdehyde (1,4-bis[(5-*tert*-butyl-3-formyl-4-hydroxyphenyl)ethynyl]benzene)<sup>[18]</sup> and the ex situ synthesis of the diimine (1,4-bis[(5-*tert*-butyl-3-octylimino-4-hydroxyphenyl)ethynyl]benzene) can be found in the Supporting Information. The compounds were evaporated from a heated glass crucible. Octylamine (99%, Aldrich) was held in a glass vial and dosed through a leak valve.

For the in situ reaction (for STM imaging), a subsaturation coverage of the dialdehyde (typically less than 1/3 monolayer, as estimated by STM) was formed by deposition on a sample held at room temperature. Subsequently, the sample was nearly saturated with octylamine by dosing for 1–2 min at a pressure of  $1\text{--}5 \times 10^{-8}$  mbar, while the sample was held at room temperature. To complete the reaction and to enhance the order on the surface, the



sample was annealed at temperatures in the range of 400–450 K. The order of the deposition of the reactants did not influence the outcome. For imaging, the STM was cooled to temperatures in the range of 120–160 K.

NEXAFS spectra were obtained at the beamline HE-SGM at BESSY II. The reference spectra shown in Figure 2 were obtained for a saturated monolayer of octylamine (deposition of multilayer at 108 K and subsequent heating to 260 K), a saturated monolayer of the dialdehyde (deposition of multilayer at room temperature and subsequent heating to 435 K), and a multilayer of the diimine. For the in situ reaction,  $\frac{1}{3}$  of the saturation coverage of the dialdehyde was evaporated (coverage determined using X-ray photoelectron spectroscopy (XPS)), and the sample was subsequently cooled to 239 K and exposed to octylamine (27 Langmuir), resulting in the adsorption of a multilayer of octylamine. The sample was then annealed at 410 K to desorb multilayers and complete the reaction. The peak assignment was made based on the peak positions from the literature of 284.5 eV for aromatic carbon atoms, 286.6 eV for carbonyl carbon atoms,<sup>[14]</sup> and 285.9 eV for imine carbon atoms.<sup>[15]</sup> Small shifts of the measured peak positions as compared with those in the literature as well as between the dialdehyde and the diimine are due to the difference between a chemisorbed monolayer and a physisorbed multilayer.

All theoretical calculations were made using the DFT code DACAPO. The exchange–correlation functional PW91 was employed. The molecules were described in a large ( $17 \times 15 \times 10$  Å) supercell, and the wave functions were expanded on a basis of plane waves with energies up to 25 Ry. Ultrasoft pseudopotentials were used to describe the atomic cores. The populations of the one-electron states were stabilized by a broadening of the states according to Fermi statistics at  $k_B T = 0.1$  eV. The reaction energy pathways and transition states were determined using the climbing nudged elastic band (CNEB) method. The positions of the  $N = 48$  atoms in the setup were optimized until the  $3N$  norms of the  $3N$  forces perpendicular to the individual reaction paths were smaller than  $0.2 \text{ eV Å}^{-1}$  or until the energy barrier was insignificant compared to the barriers along other parts of the reaction paths.

Received: June 27, 2007

Revised: August 17, 2007

Published online: October 29, 2007

**Keywords:** adsorption · imines · scanning probe microscopy · self-assembly · surface chemistry

- [2] a) S. Berner, M. Brunner, L. Ramoino, H. Suzuki, H. J. Güntherodt, T. A. Jung, *Chem. Phys. Lett.* **2001**, 348, 175; b) T. Yokoyama, S. Yokoyama, T. Kamikado, Y. Okuno, S. Mashiko, *Nature* **2001**, 413, 619.
- [3] J. A. Theobald, N. S. Oxtoby, M. A. Phillips, N. R. Champness, P. H. Beton, *Nature* **2003**, 424, 1029.
- [4] M. Stöhr, M. Wahl, C. H. Galka, T. Riehm, T. A. Jung, L. H. Gade, *Angew. Chem.* **2005**, 117, 7560; *Angew. Chem. Int. Ed.* **2005**, 44, 7394.
- [5] A. Dmitriev, H. Spillmann, N. Lin, J. V. Barth, K. Kern, *Angew. Chem.* **2003**, 115, 2774; *Angew. Chem. Int. Ed.* **2003**, 42, 2670.
- [6] a) Y. Okawa, M. Aono, *Nature* **2001**, 409, 683; b) S. W. Hla, L. Bartels, G. Meyer, K. H. Rieder, *Phys. Rev. Lett.* **2000**, 85, 2777.
- [7] a) O. Endo, H. Ootsubo, N. Toda, M. Suhara, H. Ozaki, Y. Mazaki, *J. Am. Chem. Soc.* **2004**, 126, 9894; b) J. M. Bonello, R. M. Lambert, N. Kunzle, A. Baiker, *J. Am. Chem. Soc.* **2000**, 122, 9864; c) S. Lavoie, M.-A. Laliberté, G. Mahieu, V. Demers-Carpentier, P. McBreen, *J. Am. Chem. Soc.* **2007**, 129, 11668.
- [8] a) G. S. McCarty, P. S. Weiss, *J. Am. Chem. Soc.* **2004**, 126, 16772; b) J. Ma, B. L. Rogers, M. J. Humphry, D. J. Ring, G. Goretzki, N. R. Champness, P. H. Beton, *J. Phys. Chem. B* **2006**, 110, 12207.
- [9] E. H. Cordes, W. P. Jencks, *J. Am. Chem. Soc.* **1962**, 84, 832.
- [10] a) S. F. Alvarado, W. Riess, M. Jandke, P. Strohhriegl, *Org. Electron.* **2001**, 2, 75; b) X. D. Wang, K. Ogino, K. Tanaka, H. Usui, *Thin Solid Films* **2003**, 438, 75.
- [11] a) S. Haq, N. V. Richardson, *J. Phys. Chem. B* **1999**, 103, 5256; b) A. Götzhauser, S. Panov, M. Mast, A. Schertel, M. Grunze, C. Wöll, *Surf. Sci.* **1995**, 334, 235.
- [12] M. Nielsen, A. H. Thomsen, T. R. Jensen, H. J. Jakobsen, J. Skibsted, K. V. Gothelf, *Eur. J. Org. Chem.* **2005**, 342.
- [13] a) S. Weigelt, C. Busse, L. Petersen, E. Rauls, B. Hammer, K. V. Gothelf, F. Besenbacher, T. R. Linderth, *Nat. Mater.* **2006**, 5, 112; b) C. Busse, S. Weigelt, L. Petersen, E. Lægsgaard, F. Besenbacher, T. R. Linderth, A. H. Thomsen, M. Nielsen, K. V. Gothelf, *J. Phys. Chem. B* **2007**, 111, 5850.
- [14] A. B. Sherrill, V. S. Lusvardi, J. Eng, J. G. G. Chen, M. A. Barteau, *Catal. Today* **2000**, 63, 43.
- [15] A. G. Shard, J. D. Whittle, A. J. Beck, P. N. Brookes, N. A. Bullett, R. A. Talib, A. Mistry, D. Barton, S. L. McArthur, *J. Phys. Chem. B* **2004**, 108, 12472.
- [16] N. E. Hall, B. J. Smith, *J. Phys. Chem. A* **1998**, 102, 4930.
- [17] E. Lægsgaard, F. Besenbacher, K. Mortensen, I. Stensgaard, *J. Microsc.* **1988**, 152, 663.
- [18] K. V. Gothelf, A. H. Thomsen, M. Nielsen, R. S. Brown, WO2004050231, **2004**.

[1] M. C. Blüm, E. Cavar, M. Pivetta, F. Patthey, W. D. Schneider, *Angew. Chem.* **2005**, 117, 5468; *Angew. Chem. Int. Ed.* **2005**, 44, 5334.